



Cite this: *New J. Chem.*, 2014, **38**, 4594

Received (in Montpellier, France)
24th April 2014,
Accepted 26th June 2014

DOI: 10.1039/c4nj00652f

www.rsc.org/njc

Synthesis of Pd(II) organometal incorporated ordered *Im3m* mesostructural silica and its catalytic activity in a water-medium Sonogashira reaction

Fengxia Zhu, Lili Zhu, Xiaojun Sun, Litao An,* Pusu Zhao* and Hexing Li

A novel and reusable Pd(II) organometal functionalized SBA-16 catalyst was synthesized by the co-condensation of Pd[PPh₂(CH₂)₂Si(OCH₂CH₃)₃Cl₂ and tetraethyl orthosilicate (TEOS). This catalyst possessed bicontinuous cubic *Im3m* mesostructure channels, which ensured the convenient diffusion of the reactant molecules into the pore channels. The catalyst exhibited a very high activity for the Sonogashira coupling reaction of aryl halides with phenylacetylene in water medium. Moreover, the synthesized catalyst could be separated from the reaction mixture by simple filtration and reused for up to five runs without significant loss in activity.

1. Introduction

The Sonogashira coupling reaction of acetylene with aryl halides catalyzed by Pd(II) complexes is a powerful tool in organic synthesis and has been widely applied in various areas including biologically active molecules, natural product synthesis and materials science.^{1–4} This reaction is usually performed in a homogeneous system with an organic solvent and a palladium-phosphorous complex.^{5–7} The use of toxic organic solvents such as DMSO, DMF, acetonitrile, *etc.* in the Sonogashira coupling reaction not only increases the cost of the experiment, but also pollutes the environment. Water is cheap, nontoxic, and nonflammable which could be considered as an alternative to expensive organic solvents and an attractive media for the development of environmentally harmless chemical processes. Furthermore, the separation of water-insoluble organic compounds from the aqueous phase is very easy in many cases.⁸

Recently, homogenous Pd complex catalysts have also been employed in water-medium organic reactions, which could diminish environmental pollution from organic solvents.^{9,10} Despite the high activity and selectivity of homogeneous palladium organometallic catalysts there are disadvantages regarding separation and recycling. Moreover, the reaction suffers from severe problems related to the separation, recovery, and recycling of the expensive toxic metal catalysts, *etc.*¹¹

In this regard, different types of heterogeneous catalysts have been prepared with the aim of achieving catalyst recovery and recycling for the water-medium Sonogashira coupling

reaction. Examples include PVC-supported Pd nanoparticles,¹² a polystyrene resin-supported Pd(II) complex catalyst,¹³ a polymer supported macrocyclic Schiff base palladium complex,¹⁴ organopalladium(II) immobilized silicas,¹⁵ and so on.

It is obvious that the functionalized supports are used to immobilize palladium complex catalysts, which show higher activities than homogeneous catalysts in the Sonogashira coupling reaction in water.^{16–19} Among the different supports used for immobilized Pd(II) homogeneous catalysts, mesoporous silica materials remain the most popular choice because of their relatively low cost, large surface area, high thermal stability, mechanical stability, and good catalytic performance.²⁰ SBA-15 and MCM-41 are representative examples of these types of materials and have been used as supports for palladium catalysts.^{17,21–23}

Compared with two-dimensional hexagonal mesoporous materials such as SBA-15, the mesoporous material SBA-16 (cubic, *Im3m*)²⁴ is a new possible solid support for the immobilization of heterogeneous catalysts. The large surface area and interesting 3D structure, consisting of ordered and interconnected spherical mesopores, make it easily accessible for guest molecules, which facilitate the transport of reactants and products without pore blockage.^{25–28} Up to now, most SBA-16 supported Pd heterogeneous catalysts have been prepared by either post-grafting or impregnation methods, while the organic functionalities terminally bonded to the pore surface might partially block the pore channels, which might negatively affect the catalytic efficiency.^{28,29} Moreover, they could easily suffer from leaching during liquid phase reactions, leading to poor durability.²⁹

In this paper, we report the synthesis of functionalized SBA-16 with Pd(II) organometal incorporated into silica framework by

Jiangsu Key Laboratory for Chemistry of Low-Dimensional Materials, Huaiyin Normal University, Huaian, 223300, P. R. China. E-mail: anlitao@hotmail.com, zhaopusu66@sohu.com; Fax: +86 517 83525083; Tel: +86 517 83525377

surfactant-directed co-condensation between tetraethoxysilane (TEOS) and Pd(II)organometallicsilane. This functionalized mesoporous material not only acts as an effective palladium catalyst for the water-medium Sonogashira coupling reaction, but can also be reused five times without an obvious loss of catalytic activity. Its activity is higher than the analogous catalysts which are prepared from SBA-15.

2. Experimental

2.1. Catalyst preparation

Firstly, the Pd[PPh₂(CH₂)₂Si(OCH₂CH₃)₃]₂Cl₂ was synthesized by mixing 10 mL of toluene, 3.5 mmol of Pd(COD)Cl₂ and 0.70 mmol of PPh₂CH₂CH₂Si(OCH₂CH₃)₃ under argon atmosphere, followed by stirring at 30 °C for 3 h. After being concentrated to 6.0 mL pentane was added, leading to Pd[PPh₂-(CH₂)₂Si(OCH₂CH₃)₃]₂Cl₂. Then, the organopalladium(II) functionalized SBA-16, denoted as Pd(II)-PMO-SBA-16, was prepared using the co-condensation method. In a typical synthesis, 1.0 g of F127 and 2.6 g of K₂SO₄ was dissolved in 30 g of 0.50 M HCl solution with stirring at 38 °C. After complete dissolution, 4.5 g of tetraethyl orthosilicate (TEOS) was added to the homogeneous solution. After being prehydrolyzed for 1 h, 0.42 g of Pd[PPh₂-(CH₂)₂Si(OCH₂CH₃)₃]₂Cl₂ was added into the solution. This mixture was left under vigorous stirring at 38 °C for 24 h. Subsequently, hydrothermal treatment of the reactant mixture was carried out at 100 °C for 24 h under static conditions in a closed polypropylene bottle. Finally, the surfactants and other organic substances were extracted by refluxing in ethanol solution at 80 °C for 24 h. The Pd(II) loading was determined as 3.2 wt% by ICP analysis.

For comparison, the organopalladium(II) functionalized SBA-15, denoted as Pd(II)-PMO-SBA-15 was also prepared by surfactant-directed co-condensation of Pd[PPh₂(CH₂)₂Si(OCH₂CH₃)₃]₂Cl₂ and TEOS. Briefly, 0.5 g of P123 was dissolved in 15 g of 2.0 M HCl solution and 3.9 g of distilled water, 1.0 g of TEOS was added at 40 °C. After being prehydrolyzed for 1 h, 0.14 g of Pd[PPh₂(CH₂)₂Si(OCH₂CH₃)₃]₂Cl₂ was added into the solution. The mixture was left under stirring for 24 h at 40 °C, and subsequently heated for another 24 h at 100 °C under static conditions in a closed polypropylene bottle. The yellow solid product was collected and extracted in ethanol solution at 80 °C. The Pd(II) loading was determined as 2.9 wt% by ICP analysis.

2.2. Characterization

The compositions and Pd(II) loadings were determined using elemental analysis (Elementar Vario ELIII, Germany) and an inductively coupled plasma optical emission spectrometer (ICP-OES, Varian VISTA-MPX). Fourier transform infrared (FTIR) spectra were collected using a Nicolet Magna 550 spectrometer and the KBr method. Solid-state NMR spectra were recorded using a Bruker AV-400 spectrometer. Thermogravimetric analysis and differential thermal analysis (TG/DTA) were conducted using a DT-60. Low-angle X-ray powder diffraction (XRD) patterns were obtained using a Rigaku D/maxr B diffractometer with Cu K α .

N₂ adsorption-desorption isotherms were measured at 77 K using a Quantachrome NOVA 4000e analyzer, from which the specific surface area (*S*_{BET}) was calculated by applying the Brunauer-Emmett-Teller (BET) method and Barrett-Joyner-Halenda (BJH) model to the adsorption branches. Meanwhile, the average pore diameter (*D*_p) and total pore volume (*V*_p) were calculated from the adsorption isotherms using the Barrett-Joyner-Halenda (BJH) model. The surface morphologies and porous structures were observed using transmission electron microscopy (TEM, JEOL JEM2011). The surface electronic states were analyzed using X-ray photoelectron spectroscopy (XPS, Perkin-Elmer PHI 5000C). All the binding energy (BE) values were calibrated by using the standard BE value of contaminant carbon (*C*_{1s} = 284.6 eV) as a reference.

2.3. Activity test

A mixture of aryl halide (1.0 mmol), phenylacetylene (1.5 mmol), 1,8-diazabicyclo [5.4.0] undec-7-ene (DBU, 0.40 mL), CuI (0.16 mmol), *n*-decane (2.0 mmol) as an internal standard, H₂O (4.0 mL) and the catalyst with Pd(II) (0.0060 mmol), was stirred in a flask at 90 °C for a given time (Scheme 1). After the reaction was complete, the products were extracted with acetic ether, followed by analysis using a gas chromatograph (SHIMADZU, GC-17A) equipped with a JWDB-5, 95% dimethyl 1-(5%)-diphenylpolysiloxane column and a FID detector. The column temperature was programmed from 80 to 250 °C at a ramp speed of 10 °C min⁻¹. N₂ was used as carrier gas. The reproducibility was checked by repeating each result at least three times and was found to be within $\pm 5\%$.

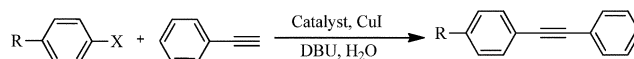
2.4. Catalyst recycling

A mixture of iodobenzene (1.0 mmol), phenylacetylene (1.5 mmol), DBU (0.40 mL), CuI (0.16 mmol), H₂O (4.0 mL) and Pd(II)-PMO-SBA-16 was stirred at 90 °C. At the end of the reaction, the mixture was cooled to room temperature and filtered to obtain the Pd(II)-PMO-SBA-16 catalyst. The separated catalyst was washed with ethanol and dried under vacuum at 60 °C. The catalyst was separated from the liquid phase by high-speed centrifugation. After this, the catalyst was reused with a fresh charge of reactants for subsequent recycling under identical reaction conditions.

3. Results and discussion

3.1. Structural characteristics

As mentioned in the experimental, the Pd[PPh₂(CH₂)₂Si(OCH₂CH₃)₃]₂Cl₂ was prepared from Pd(COD)Cl₂ and PPh₂CH₂CH₂Si(OCH₂CH₃)₃ under argon protection. Then, the organopalladium(II) functionalized SBA-16, denoted as Pd(II)-PMO-SBA-16, was prepared by co-condensation from the



Scheme 1 Chemical equation of the Sonogashira coupling reaction between aryl halide and phenylacetylene.

obtained Pd[PPh₂(CH₂)₂Si(OCH₂⁻CH₃)₂Cl₂ and tetraethyl ortho-silicate (TEOS). Pd(II)-PMO-SBA-16 and Pd(II)-PMO-SBA-15 were almost 2 μm in length and 500 nm in diameter. They were determined using SEM analysis.

Elemental analysis showed that the Pd[PPh₂(CH₂)₂Si(OCH₂⁻CH₃)₂Cl₂ sample had a composition of C (55.24%) and H (6.57%), which is in good accordance with that calculated for C₆₀H₈₇O₉Cl₂P₃PdSi₃ (C (55.18%) and H (6.67%)). ICP analysis showed a P/Pd molar ratio of 2.03. The Pd(II) organometallic complex incorporated into the silica matrix by the co-condensation approach was investigated using FTIR, solid-state NMR, and TG-DTA. Fig. 1 shows the FTIR spectra of Pd(II)-PMO-SBA-16. No significant signals indicative of P123 surfactant molecules were observed, implying that they were completely removed during EtOH extraction. There are two peaks corresponding to Pd(II)-PMO-SBA-16, shown at 2985 and 2919 cm⁻¹, which could be attributed to the asymmetric and symmetric stretching modes of C–H bonds.³⁰ The peak at 693 cm⁻¹ is characteristic of the –H out-of-plane deformation of the monosubstituted benzene ring. The peak around 1436 cm⁻¹ was assigned to the vibrations of P–CH₂.³¹ These results confirm the successful incorporation of the Pd(II) organometallic complex into the silica supports. The absorption peak at 1130–1090 cm⁻¹ which is indicative of the P–Ph vibration could not be clearly distinguished due to the overlap with the intense Si–O vibration bands at 1100 cm⁻¹.³⁰ The incorporation of the Pd(II) organometallic complex into the SBA-16 network could be further characterized using the solid-state NMR spectra.

As shown in Fig. 2, the ¹³C CPMAS NMR spectrum of the Pd(II)-PMO-SBA-16 sample displays two peaks at 14 and 57 ppm which were assigned to the two C atoms in the –CH₂–CH₂–PPh₂ group. A broad peak around 128 ppm was assigned to the C atoms in the benzene ring.^{32,33} Meanwhile, the ²⁹Si MAS NMR spectrum of the Pd(II)-PMO-SBA-16 sample displayed three resonance peaks up-field corresponding to Q⁴ (δ = –112 ppm), Q³ (δ = –102 ppm), and Q² (δ = –94 ppm) and two peaks down-field corresponding to T³ (δ = –66 ppm) and T² (δ = –59 ppm), where Qⁿ = Si(OSi)_n–(OH)_{4–n}, n = 2–4, and T^m = RSi(OSi)_m–(OH)_{3–m}, m = 1–3.³³ The presence of T^m peaks suggest that the organic silica moieties were successfully incorporated as a part of the silica wall structure.

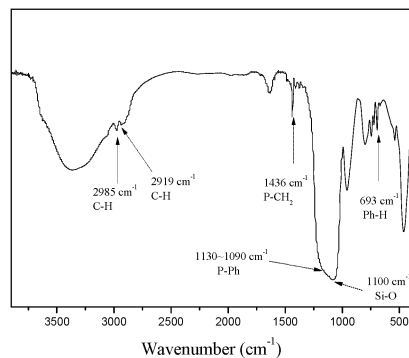


Fig. 1 FTIR spectra of Pd(II)-PMO-SBA-16.

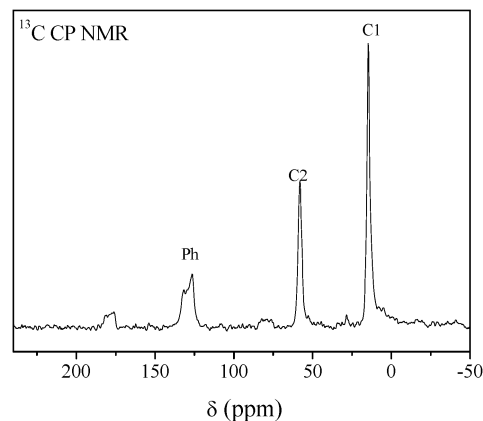
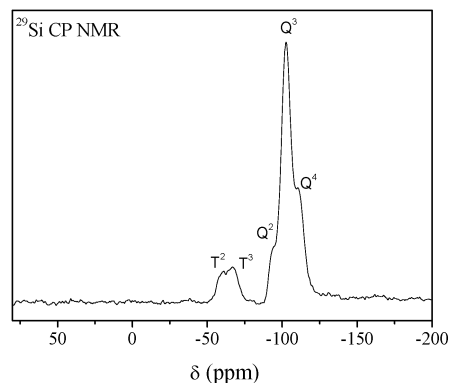


Fig. 2 Solid NMR spectra of Pd(II)-PMO-SBA-16.

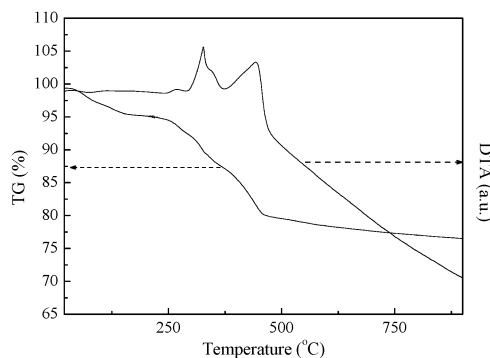


Fig. 3 TG and DTA curves of Pd(II)-PMO-SBA-16.

This was further confirmed by the TG/DTA. As shown in Fig. 3, besides the weight loss due to the removal of physisorbed water, and/or remaining ethanol from the solvent extraction processes, the Pd(II)-PMO-SBA-16 displayed two peaks around 383 and 452 °C. These peaks are possibly due to the successive breakage of two PPh₂–Pd–PPh₂ bonds,²⁴ corresponding to a total weight loss of around 16%.

As shown in Fig. 4, the XPS spectra show that all the Pd species in the Pd(II)-PMO-SBA-16 were present in a +2 oxidation state rather than in a metallic state, corresponding to the binding energy (BE) of 343.1 and 337.8 eV in the Pd 3d_{5/2} and

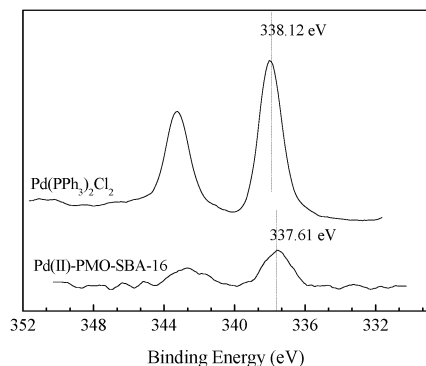


Fig. 4 XPS spectra of Pd(PPh₃)₂Cl₂ and Pd(II)-PMO-SBA-16.

3d_{3/2} levels,³⁴ respectively. In comparison with the BE of Pd in Pd(PPh₃)₂Cl₂, the BE of Pd in Pd(II)-PMO-SBA-16 shifted negatively by 0.51 eV, indicating that the PPh₂CH₂CH₂-ligand exhibited stronger electron-donation than the PPh₃-ligand, making the Pd atom in the Pd(II)-PMO-SBA-16 more electron-enriched. This can be easily understood by considering the conjugated π - π system between P and Ph-. The PPh₃-ligand exhibits a conjugated π - π system comprising one P atom and three Ph groups while the PPh₂-CH₂-CH₂-ligand exhibits a conjugated π - π system comprising one P atom and two Ph groups.²⁹ The bigger conjugated π - π system might dilute the electron density on the P atom, which weakens the electron donation ability of the P atom to the Pd atom in the coordination bonds.³²

The small-angle XRD pattern of Pd(II)-PMO-SBA-16 in Fig. 5 exhibits a significant peak at 0.7° corresponding to the (110) reflection and comparatively unresolved peaks at 2 θ values in the range of 1.0°–2.0°. These peaks are related to the *Im3m* body-centered cubic space group, thus providing an indication of the *Im3m* structure of SBA-16.³⁵ The TEM images (Fig. 6) further confirmed the presence of the ordered cubic (space group *Im3m*) mesostructure of Pd(II)-PMO-SBA-16.

Fig. 7 illustrates the nitrogen adsorption-desorption isotherms of the Pd(II)-PMO-SBA-16 sample. The prepared sample exhibited a type IV N₂ sorption isotherm with a H₂-type hysteresis loop, which is characteristic of mesoporous materials with a cage-type porous structure, suggesting the existence of ink-bottle pores in the above sample.³⁶ The pore size distribution, calculated

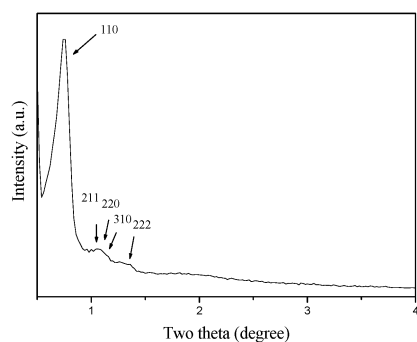


Fig. 5 Low-angle XRD pattern of Pd(II)-PMO-SBA-16.

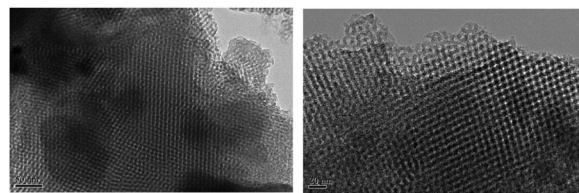


Fig. 6 TEM images of Pd(II)-PMO-SBA-16.

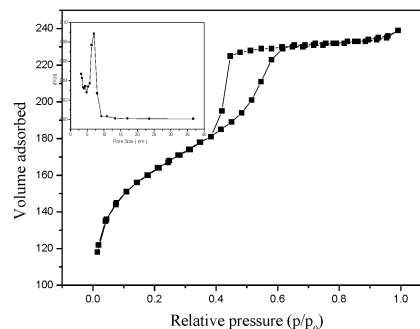


Fig. 7 N₂ adsorption-desorption isotherms of Pd(II)-PMO-SBA-16 and pore size distribution curves (inset).

using the adsorption branch of the N₂ isotherm with the Barrett-Joyner-Halenda method (Fig. 7 inset), shows that the primary mesopores of SBA-16 have a diameter of 6.4 nm, with the volume of mesopores and the specific surface area estimated to be 0.51 cm³ g⁻¹ and 676 m² g⁻¹, respectively.

A key consideration of the Pd(II)-PMO-SBA-16 catalyst is the location of the Pd(II) species since they should come into contact with reactant molecules. To determine the chemical accessibility of the Pd(II) organometals incorporated into the silica framework, the oxidation of Pd(II)-PMO-SBA-16 in KMnO₄ aqueous solution was attempted. The Pd(II) content, determined by KMnO₄ oxidation, could be considered as an accessible Pd(II) species, while the total Pd(II) content was determined using ICP analysis. Their molar ratio was determined as 92%, suggesting that most of the Pd(II) species in the Pd(II)-PMO-SBA-16 catalyst were accessible for the chemical in the liquid phase reaction.

3.2. Catalytic performances

In order to test the catalytic activity of Pd(II)-PMO-SBA-16 in the Sonogashira coupling reaction, the reaction between iodobenzene and phenylacetylene was chosen as a model reaction, using water as the solvent to investigate the influence of different parameters on the catalytic activity. The parameters included the catalyst, catalyst concentration, base, and reaction temperature. The best result was obtained when the cross-coupling was carried out with 0.6 mol% of Pd(II)-PMO-SBA-16 (Table 1, entry 2). The optimized reaction conditions were then applied to the Sonogashira cross coupling reactions of various aryl halides with phenylacetylene (Table 3).

The catalytic parameters of different Pd(II) organometallic catalysts in the water-medium Sonogashira reaction are summarized in Table 2. The Pd(II)-PMO-SBA-16 displayed a comparable

Table 1 The cross-coupling of iodobenzene and phenyl-acetylene under different conditions^a

Entry	Catalyst content (mol%)	Base	Temperature (°C)	Yield (%)
1	0.3	DBU	50	62
2	0.6	DBU	70	86
3	0.9	DBU	90	95
4	0.6	Et ₃ N	90	87
5	0.6	K ₂ CO ₃	90	75
6	0.3	DBU	90	51
7	0.9	DBU	90	97

^a Reactions conditions: iodobenzene (1.0 mmol), phenylacetylene (1.5 mmol), base, CuI (0.16 mmol), *n*-decane (2.0 mmol), H₂O (4.0 mL), and Pd(II)-PMO-SBA-16.

Table 2 The catalytic efficiencies of different catalysts in the water-medium Sonogashira reaction^a

Entry	Catalyst	Yield (%)
1	Pd(PPh ₃) ₂ Cl ₂	97
2	Pd(II)-PMO-SBA-16	95
3	Pd(II)-PMO-SBA-15	88

^a Reactions conditions: iodobenzene (1.0 mmol), phenylacetylene (1.5 mmol), DBU (0.40 mL), CuI (0.16 mmol), *n*-decane (2.0 mmol), H₂O (4.0 mL), 90 °C and an amount of Pd catalyst.

efficiency to the Pd(PPh₃)₂Cl₂ homogeneous catalyst. As expected, the reaction catalyzed by Pd(II)-PMO-SBA-15 had a slower rate than that of the Pd(II)-PMO-SBA-16 catalyst under the same reaction conditions. The reason could be that Pd(II)-PMO-SBA-16 has an easily accessible 3D structure consisting of ordered and interconnected spherical mesopores for guest molecules, which facilitates the transport of reactants and products without pore blockage.^{25–28}

To confirm whether the heterogeneous or the dissolved homogeneous Pd(II) species was the real catalyst responsible for the coupling reaction between iodobenzene and phenylacetylene, the following procedure was carried out, as proposed by Sheldon *et al.*³⁷ According to the proposed method, after reacting for 4 h with the conversion exceeding 45%, the solid catalyst was filtered out and the mother liquor was allowed to react for another 5 h under identical reaction conditions. No significant change in the conversion was observed, indicating that the present catalysis was indeed heterogeneous in nature rather than being due to the dissolved Pd(II) species leached from Pd(II)-PMO-SBA-16.

In order to verify the higher activity of Pd(II)-PMO-SBA-16, its activity towards aryl halide containing a variety of substituents with phenylacetylene were examined. These results are summarized in Table 3. The cross-coupling reaction of phenylacetylene with a variety of aryl iodides proceeded smoothly, affording high yields of 86–98% (Table 3, entries 1–4). Various electron-donating and electron-withdrawing groups, such as –OCH₃ and –NO₂ on the aryl iodide were well tolerated. The presence of a

Table 3 Catalytic efficiencies of the Pd(II)-PMO-SBA-16 in water-medium Sonogashira reactions^a

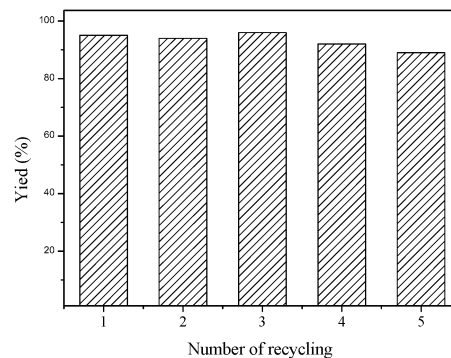
Entry	Catalyst content (mol%)	R	X	Reaction time (h)	Yield (%)
1	0.60	H	I	5	95
2	0.60	CH ₃ O–	I	7	86
3	0.60	CH ₃ –	I	7	89
4	0.60	NO ₂ –	I	4	98
5	0.90	H	Br	8	93
6	0.90	CH ₃ –	Br	10	85
7	0.90	NO ₂ –	Br	7	96

^a Reactions conditions: aryl halide (1.0 mmol), phenylacetylene (1.5 mmol), DBU (0.40 mL), CuI (0.16 mmol), *n*-decane (2.0 mmol), H₂O (4.0 mL), 90 °C and PMO-SBA-16.

strong electron-withdrawing group, such as –NO₂, is known to promote the direct coupling. Electron-donating groups, such as –OCH₃ on the iodoaryl partner gave excellent results. The results above prompted us to investigate the reaction of aryl bromides. With a catalyst loading of 0.9 mol%, Pd(II)-PMO-SBA-16 also afforded a satisfactory yield for bromides containing –CH₃ and –OCH₃ groups (Table 3, entries 5–7). Bromoarenes with either electron-withdrawing substituents, such as –NO₂, or electron-donating substituents, such as –OCH₃, coupled readily with phenylacetylene in good yields. Aryl bromides containing electron-withdrawing substituents reacted faster than those with electron donating substituents (Table 3, entries 6 and 7).

3.3. Recycling of the catalyst

One of the purposes for designing this heterogeneous catalyst is to enable the recycling of the catalyst for use in subsequent reactions. The reusability of the catalyst was tested by reacting phenyl iodide with phenylacetylene, as the representative reactants, in the presence of 0.60 mol% of Pd(II), in order to study the recyclability of this heterogeneous catalyst. Due to the unavoidable loss of solid catalyst during the course of recovery and washing, we did three parallel reactions during each cycle, then collected all the catalyst and portioned them for the next cycling. Both Pd(II)-PMO-SBA-16 and Pd(II)-PMO-SBA-15 could be reused for five cycles without a significant decrease in the catalytic activity of the catalyst (Fig. 8). The excellent durability of the

**Fig. 8** Recycling tests of Pd(II)-PMO-SBA-16.

Pd(II)-PMO-SBA-16 catalyst could be attributed to the Pd(II) organometallic complex embedded in the silica walls, which could effectively inhibit Pd(II)-leaching. According to the ICP analysis, the amount of Pd(II) species in the solution was less than 0.5 ppm after being used five times, suggesting that Pd(II)-leaching could be essentially neglected. On the other hand, the Pd(II) organometals embedded in the silica walls might also enhance the hydrothermal stability of Pd(II)-PMO-SBA-16.³⁸

4. Conclusions

In summary, we have presented a Pd(II) organometal functionalized SBA-16, which was efficiently used as a heterogeneous catalyst for Sonogashira coupling reactions in water medium. The catalyst not only shows high catalytic activity, but also offers many practical advantages such as thermal stability and recyclability. The catalyst was reused for five runs in a Sonogashira reaction without a significant loss of activity, indicating good potential for industrial applications. In comparison with those bonded to traditional mesoporous silica supports (e.g., SBA-15), the three-dimensional mesoporous cage-like material SBA-16 was demonstrated to have a superior ability in reducing the diffusion resistance. It can be envisioned that other organometallic catalysts including Rh(I), Ru(II), Ni(II), and rare earth metals can also be designed in this way, which may offer more opportunities for developing powerful and reusable catalysts for green organic synthesis.

Acknowledgements

We are grateful to the National Natural Science Foundation of China (20825724), University Natural Science Foundation of Jiangsu Province (13KJB150008) and Administration of Science & Technology of Huaian city (HAG2013077).

References

- 1 K. Sonogashira, *Metal-Catalyzed Cross-Coupling Reactions*, Wiley-VCH, New York, USA, 1998.
- 2 I. Paterson, R. D. M. Davies and R. Marquez, *Angew. Chem., Int. Ed.*, 2001, **40**, 603.
- 3 T. Hundertmark, A. F. Littke, S. L. Fu and G. C. Buchwald, *Org. Lett.*, 2000, **2**, 1729.
- 4 N. D. P. Cosford, L. Tehrani, J. Roppe, E. Schweiger, N. D. Smith, J. Anderson, L. Bristow, J. Brodtkin, X. Jiang, I. McDonald, S. Rao, M. Washburn and M. A. Varney, *J. Med. Chem.*, 2003, **46**, 204.
- 5 K. Sonogashira, Y. Tohda and N. Hagihara, *Tetrahedron Lett.*, 1975, **16**, 4467.
- 6 R. Chinchilla and C. Nájera, *Chem. Soc. Rev.*, 2011, **40**, 5084.
- 7 R. Chinchilla and C. Nájera, *Chem. Rev.*, 2007, **107**, 874.
- 8 A. N. Marziale, J. Schlüter and J. Eppinger, *Tetrahedron Lett.*, 2011, **52**, 6355.
- 9 A. Komáromi, G. L. Tolnai and Z. Novák, *Tetrahedron Lett.*, 2008, **49**, 7294.

- 10 X. Z. Wang, J. Zhang, Y. Y. Wang and Y. Liu, *Catal. Commun.*, 2013, **40**, 23.
- 11 M. O. Simon and C. J. Li, *Chem. Soc. Rev.*, 2012, **41**, 1415.
- 12 B. Basavaprabhu, M. Samarasimhareddy, G. Prabhu and V. Sureshbabu, *Tetrahedron Lett.*, 2014, **55**, 2256.
- 13 M. Bakherad, A. Keivanloo, B. Bahramian and S. Jajarmi, *J. Organomet. Chem.*, 2013, **724**, 206.
- 14 Y. He and C. Cai, *J. Organomet. Chem.*, 2011, **696**, 2689.
- 15 C. M. Kang, J. L. Huang, W. H. He and F. Zhang, *J. Organomet. Chem.*, 2010, **695**, 120.
- 16 M. J. Jin and D. H. Lee, *Angew. Chem., Int. Ed.*, 2010, **49**, 1119.
- 17 A. K. Nezhad and F. Panahi, *Green Chem.*, 2011, **13**, 2408.
- 18 Y. He and C. Cai, *J. Organomet. Chem.*, 2011, **696**, 2689.
- 19 W. H. He, F. Zhang and H. X. Li, *Chem. Sci.*, 2011, **2**, 961.
- 20 V. Polshettiwar, C. Len and A. Fihri, *Chem. Rev.*, 2009, **253**, 2599.
- 21 J. Huang and F. Zhang, *Appl. Organomet. Chem.*, 2010, **24**, 767.
- 22 E. B. Cho, D. Kim, J. Gorka and M. Jaroniec, *J. Mater. Chem.*, 2009, **19**, 2076.
- 23 A. Molnár, *Chem. Rev.*, 2011, **111**, 2251.
- 24 D. Y. Zhao, Q. Huo, J. Feng, B. F. Chmelka and G. D. Stucky, *J. Am. Chem. Soc.*, 1998, **120**, 6024.
- 25 E. Rivera-Muñoz and R. Huirache-Acuña, *Int. J. Mol. Sci.*, 2010, **11**, 3069.
- 26 Y. Sakamoto, M. Keneda, O. Teresaki, D. Y. Zhao, J. Kim and G. Stucky, *Nature*, 2000, **408**, 4493.
- 27 D. Y. Zhao, J. Feng, Q. Huo, N. Melosh, G. Fredrickson and B. Chmelka, *Science*, 1998, **279**, 548.
- 28 R. Grudzien, B. Grabicka and M. Jaroniec, *J. Mater. Chem.*, 2006, **16**, 819.
- 29 X. S. Yang, F. X. Zhu, J. L. Huang, F. Zhang and H. X. Li, *Chem. Mater.*, 2009, **21**, 4925.
- 30 A. S. M. Chong and X. S. Zhao, *J. Phys. Chem. B*, 2003, **107**, 12650.
- 31 Q. Hu, J. Hampsey, N. Jiang, C. Li and Y. Lu, *Chem. Mater.*, 2005, **17**, 1561.
- 32 F. Zhang, G. H. Liu, H. X. Li and Y. F. Lu, *Adv. Funct. Mater.*, 2008, **18**, 1.
- 33 M. Jurgen, G. Martin, W. Georg, J. Jian, H. Michael, J. Peter and F. Michael, *J. Mater. Chem.*, 2006, **16**, 2809.
- 34 J. F. Moulder, W. F. Stickle, P. E. Sobol and K. D. Bomben, *Handbook of X-ray Photoelectron Spectroscopy, A Reference Book of Standard Spectra for Identification and Interpretation of XPS Data*, Perkin-Elmer Corporation, Physical Electronics Division, Eden Prairie, MN, 1992.
- 35 H. Q. Yang, L. Zhang, W. Su, Q. Yang and C. Li, *J. Catal.*, 2007, **248**, 204.
- 36 K. Morishige, N. Tateishi and S. Fukuma, *J. Phys. Chem. B*, 2003, **107**, 5177–5181.
- 37 R. A. Sheldon, *Green Chem.*, 2005, **7**, 267.
- 38 J. E. Herrera, J. Kwak, J. Z. Hu, Y. Wang, C. H. F. Peden, J. Macht and E. Iglesia, *J. Catal.*, 2006, **239**, 200.